Burnett-Cattaneo continuum theory for shock waves

Brad Lee Holian,[1] Michel Mareschal,[2] and Ramon Ravelo[3]
[1]*Theoretical Division, Los Alamos National Laboratory, Los Alamos, New Mexico 87545, USA*
[2]*Physics Department, CP223, Université Libre de Bruxelles, B-1050 Bruxelles, Belgium*
[3]*Physics Department, University of Texas at El Paso, El Paso, Texas 79968, USA and Computational Physics Division, Los Alamos National Laboratory, Los Alamos, New Mexico 87545, USA*
(Received 9 September 2010; revised manuscript received 30 November 2010; published 10 February 2011; publisher error corrected 15 February 2011)

We model strong shock-wave propagation, both in the ideal gas and in the dense Lennard-Jones fluid, using a refinement of earlier work, which accounts for the cold compression in the early stages of the shock rise by a nonlinear, Burnett-like, strain-rate dependence of the thermal conductivity, and relaxation of kinetic-temperature components on the hot, compressed side of the shock front. The relaxation of the disequilibrium among the three components of the kinetic temperature, namely, the difference between the component in the direction of a planar shock wave and those in the transverse directions, particularly in the region near the shock front, is accomplished at a much more quantitative level by a rigorous application of the Cattaneo-Maxwell relaxation equation to a reference solution, namely, the steady shock-wave solution of linear Navier-Stokes-Fourier theory, along with the nonlinear Burnett heat-flux term. Our new continuum theory is in nearly quantitative agreement with nonequilibrium molecular-dynamics simulations under strong shock-wave conditions, using relaxation parameters obtained from the reference solution.

DOI: 10.1103/PhysRevE.83.026703 PACS number(s): 47.11.Mn, 47.40.−x, 02.70.Ns, 45.10.−b

I. INTRODUCTION

Continuum theories of hydrodynamic flow confront the most stringent test of their limits of validity in the description of shock-wave fronts. Because these inhomogeneous fronts are highly localized in both distance (a few interatomic spacings) and time (a few mean collision times), and because the hydrodynamic fields—the independent variables that describe the fluid flow—exhibit large gradients, the linear constitutive models that have traditionally been employed are stretched to the limits of their validity, requiring new generalizations, particularly for strong shocks.

Shock waves are so thin in spatial dimension and so rapid in time that their details are difficult to measure by laboratory experiments, but by the same token, they are therefore amenable to atomistic nonequilibrium molecular-dynamics (NEMD) computer simulations. The five hydrodynamic fields—two local thermodynamic variables (upon which the internal energy and pressure depend), namely, mass density ρ and temperature T, along with the three components of the local fluid velocity $\mathbf{u}$, all functions of position $\mathbf{x}$ and time t—can be obtained from NEMD simulations with appropriate initial and boundary conditions, and then compared to continuum numerical solutions under the same conditions. The continuum equations of change are generally expressed as partial time derivatives of the densities of mass, momentum, and energy, which are equal to negative gradients of their respective fluxes. To close the continuum equations, that is, to solve for the hydrodynamic fields, constitutive equations for forces and fluxes are invoked.

The most venerable constitutive models arrived in the momentous year 1822, when Claude-Louis Navier proposed the Navier-Stokes equations for viscous fluid flow, and his mentor, Joseph Fourier, proposed Fourier's law of heat conduction. Both together, known as Navier-Stokes-Fourier (NSF) hydrodynamics, relate fluxes to forces (i.e., gradients of the hydrodynamic fields); in the case of momentum, the pressure tensor components are proportional to negative gradients of fluid velocity, with the proportionality (transport) coefficients being bulk viscosity (η_V) and shear viscosity (η_S); in the case of energy, the heat-flux vector is proportional to the negative gradient of the temperature, with the proportionality coefficient being the thermal conductivity (κ). Equilibrium molecular-dynamics simulations are able to generate, as functions of density and temperature, both the equation of state (or EOS, namely, pressure and energy), and the limiting, zero-gradient transport coefficients (though the latter are more efficiently generated by homogeneous, steady-state NEMD simulations).

In a previous study of ours [1], we compared earlier NEMD strong-shock simulations in the dilute (ideal) gas limit [2] to NSF continuum theory, augmented by the Holian-Mareschal (HM) heat-flux vector containing (i) a higher-order term—the dominant Burnett correction, namely, the product of gradients of velocity and temperature—and (ii) an approximate relaxation term. The extension of these ideal-gas results (where only kinetic-energy terms are involved) to dense fluids (where potential-energy contributions are significant) is complicated by the difficulty of generalizing the Boltzmann equation. In a follow-up study of ours [3], we compared NEMD simulations of strong shocks in the dense Lennard-Jones (LJ) fluid to HM theory; earlier NEMD studies were compared to NSF theory [4], which had been deemed only moderately successful. We now take our second study one step further in this present paper, where our continuum theory includes an additional relaxation time integration and thereby comes very close to full agreement with NEMD in both ideal gas and dense fluids.

In both our previous papers [1,3], there were five important NEMD observations that we made:

(1) In the shock front, there is an absence of equipartition among the three spatial components of local peculiar kinetic

energy (i.e., kinetic energy measured relative to the center-of-mass fluid velocity in a local volume), which can be expressed as diagonal kinetic temperature-tensor components, by analogy with the pressure tensor. In the remainder of the paper, because we are dealing with far-from-equilibrium states, we identify the average kinetic temperature T as the local hydrodynamic field in continuum theories, and define it in terms of this local peculiar kinetic energy; hence T is one-third the trace of the kinetic temperature tensor. (In other nonequilibrium situations, different authors have employed alternative measures of the effective temperature [5]; however, in atomistic dynamics, definitions of instantaneous temperature other than kinetic are either difficult or impossible to evaluate in all circumstances.)

(2) In the shock front, the kinetic temperature component in the direction of shock propagation, T_{xx}, is higher than the transverse components, T_{yy} and T_{zz}, which are equal to each other by symmetry in the long-time average and for sufficiently large cross-sectional areas. Therefore T is also always lower than T_{xx}, except at equilibrium, which occurs long before the shock has arrived and long afterwards, when equipartition holds. Moreover, T_{xx} shows a distinct peak near the center of the shock front, and this disequilibrium is due to collisions in the shock compression process [1,3] (see also Holian *et al.* [4]).

(3) Compared to NEMD, the early-time rise of the shock front (on the cold, pre-shocked side) is seen to be too slow in NSF continuum theory, so we proposed incorporating Burnett nonlinearity into the HM heat-flux vector [1,3], characterized by a dimensionless parameter $\delta_1 \geqslant 0$ that we can estimate from ideal-gas kinetic theory.

(4) There is a relaxation process that brings the (compressional) longitudinal kinetic temperature T_{xx} back into equilibrium with the average T on a time and distance scale approximately equal to the width of the shock front. The relaxation of the pressure-tensor component in the shock direction P_{xx} to its spatial average P, which, to a very good approximation, is proportional to $T_{xx} - T$, motivated an additional temperature-relaxation term in the HM heat-flux vector, characterized by a second dimensionless parameter $\delta_2 \geqslant 0$. These two new HM augmentations to the NSF heat-flux vector do a much better job of describing NEMD shock-wave results [1,3]. (When $\delta_1 = \delta_2 = 0$, the NSF linear continuum theory is recovered from HM.)

(5) Compared to NEMD, however, the final approach toward equilibrium (on the hot, shocked side) is seen to be too rapid in earlier continuum theories (NSF and HM), both of which involved direct, one-pass integrations [1,3]. Thus we are motivated to seek a more complete theory of relaxation.

In the next section, we outline the important differences that distinguish NEMD simulations of shock waves from the usual atomistic computer simulations, and then lay out the continuum equations we solve for our reference (unrelaxed) solution. In Sec. III, we set forth our generalized Cattaneo-Maxwell relaxation approach, which requires a second time integration of the hydrodynamic fields over their past history to achieve the final, relaxed continuum theory. Sec. IV reports the results of comparing NEMD shock-wave profiles to both reference and relaxed continuum solutions, followed by the Conclusions section.

II. SHOCK-WAVE PROFILES: ATOMISTIC SIMULATIONS VS THE REFERENCE CONTINUUM SOLUTION

A steady-state, planar, left-running shock wave can be described by a profile coordinate variable, $x = X + u_s t$, where X is the initial fixed laboratory coordinate of a given mass element relative to the initial position of the piston, and the shock front is stationary at $x = 0$. Thus for a mass element at fixed X, time flies like x, namely, $t = (x - \mathrm{X})/u_s$, in the steady profile. In the reference frame of the moving shock front at $x = 0$, cold material streams in from the left at fluid velocity u_s and stagnates as hotter, denser material at the piston, which recedes at velocity $u_s - u_p$. For steady-state planar shock waves, the 5 hydrodynamic fields are reduced to 3: density ρ, the component of velocity u in the shock propagation direction (x), and the temperature T. Because the gradients of fluxes (mass, momentum, and energy) are zero in the steady state, the density becomes a function of the fluid velocity, and the three hydrodynamic fields are thereby reduced to 2: u and T. NEMD shock-wave profiles are transformed into this shock-front reference frame for comparison to the reference continuum solution.

NEMD simulations of shock waves differ from other nonequilibrium atomistic applications in five distinct ways (see Ref. [3] for more details on NEMD methodology):

(1) Momentum-mirror boundary conditions are used to generate shock waves. For example, the right-hand mirror boundary of the computational cell is moved leftward at constant piston velocity $-u_p$, generating a leftward-moving shock wave as atoms collide with the mirror; the shock velocity $-u_s$ outraces the moving mirror (piston).

(2) Shock-wave profiles are generated by lumping particles into constant-mass (Lagrangian) bins—slabs along the x direction—and computing all the variables and fluxes that appear in the various flavors of continuum theory.

(3) The steady-state transformation to the reference frame of the shock front is then applied to the NEMD profiles. Once transients have decayed, steady profiles at snapshots in time can be further averaged, so as to reduce statistical fluctuations.

(4) Density, velocity, and temperature are all point functions and are unambiguous in their atomistic interpretation; however, pressure-tensor components and energy involve potential-energy contributions that are nonlocal, due to long-range intermolecular interactions, and care must be taken to check that steady shock waves have constant mass, momentum, and energy fluxes. (In general, we find that sharing bonds equally across different bins is sufficient.)

(5) The computational time step must be sufficiently small, in order that collisions are accurately resolved in the NEMD integration.

The linear Navier-Stokes (and Fourier) constitutive "laws" of viscous flow and thermal conduction relate fluxes of momentum in the shock direction P_{xx} and heat Q to the gradients of fluid velocity du/dx and temperature dT/dx, respectively, through the transport coefficients of viscosity and thermal conductivity, thereby augmenting the Euler equations of change that describe a step-function jump (Hugoniot) from cold, unshocked material to hot, shocked material, as obtained from the local equilibrium EOS. In the continuous shock rise predicted by NSF theory, the transport coefficients are also

functions of density and temperature, and noticeably so for strong shock waves. (For HM, there is an additional Burnett-like strain-rate contribution to the thermal conductivity, but it, too, relies on the local thermodynamic collision time from the EOS.)

Starting with the continuity equation for conservation of mass, $\partial\rho/\partial t + (\partial/\partial x)(\rho u) = 0$, and the steady-state condition, $\partial\rho/\partial t = 0$, we see that the mass flux ρu is constant in a steady planar shock wave, so that u is proportional to the volume per unit mass, and the density is given by

$$\rho(x) = \frac{\rho_0 u_s}{u(x)}. \tag{1}$$

Similarly, the hydrodynamic equation of change for conservation of momentum, $\partial(\rho u)/\partial t + (\partial/\partial x)(P_{xx} + \rho u^2) = 0$, implies that the xx component of the pressure tensor in a steady planar shock wave is given by

$$P_{xx}(x) = P(\rho,T) - \eta_L(\rho,T)\frac{du}{dx} = P_0 + \rho_0 u_s^2\left(1 - \frac{u}{u_s}\right), \tag{2}$$

where the longitudinal viscosity $\eta_L = \eta_V + (4/3)\eta_S$, and P is the isotropic equilibrium pressure from the EOS (P_0 is the value in the initial, unshocked state). Note that P_{xx} and u are linear functions of each other. Since the fluid velocity (properly scaled by the shock velocity) is the volume per unit mass (scaled by the initial value), the second equality in Eq. (2) is the so-called pressure-volume Rayleigh line, the area under which is the internal energy change through the shock process.

Finally, the hydrodynamic equation of change for conservation of energy, $\partial[\rho(E + u^2/2)]/\partial t + (\partial/\partial x)[\rho u(E + u^2/2) + P_{xx}u + Q] = 0$, implies that the heat-flux vector Q (evaluated here for the HM constitutive theory [1,3]) for the steady planar shock wave is given by

$$\begin{aligned} Q(x) &= -\kappa(\rho,T)\left[1 - \delta_1\tau_c(\rho,T)\frac{du}{dx}\right]\frac{dT}{dx} - \delta_2(P_{xx} - P)u \\ &= -\rho_0 u_s\left[E(\rho,T) - \frac{1}{2}(u_s - u)^2 - E_0 \right. \\ &\quad \left. - \frac{P_0}{\rho_0}\left(1 - \frac{u}{u_s}\right)\right], \end{aligned} \tag{3}$$

where E is the internal energy from the EOS (E_0 is the value in the initial, unshocked state), the mean collision time is $\tau_c = \eta_L/B_S$, which can be calculated from the longitudinal viscosity and the EOS (the isentropic bulk modulus is B_S), and δ_1 is the dimensionless Burnett parameter. (For the HM theory we employ as a reference continuum solution in this paper, the relaxation parameter is chosen to be $\delta_2 \equiv 0$, since larger values did not sufficiently well account for the slow approach to the hot, final state, as seen in NEMD [1,3].)

NSF and HM continuum theories assume local thermodynamic equilibrium throughout the shock-wave profile; no mention is made in *any* continuum theory of the truly nonequilibrium variable T_{xx}, the temperature in the direction of the shock that arises from rapid uniaxial compression. In Ref. [3], we showed that, to a very good approximation in the dense fluid (and *exactly* in the case of the ideal gas), we could compute T_{xx} from (i) the average over the three components of the kinetic temperature T (which we use, along with ρ, to obtain the EOS), (ii) P_{xx}, and (iii) P (from the EOS):

$$T_{xx} \cong T + \left(\frac{\partial T}{\partial P}\right)_\rho(\rho,T)\,[P_{xx} - P(\rho,T)], \tag{4}$$

where the thermodynamic derivative $(\partial T/\partial P)_\rho = 1/(\partial P/\partial T)_\rho$ from the EOS is approximately linear in fluid velocity u throughout the shock wave profile. We emphasize that the kinetic temperature components in the shock front are mechanically well defined at every point and easily measured in atomistic simulations; it is only via Eq. (4) that their relationship to the local thermodynamic temperature from the equilibrium EOS can be obtained for NSF and HM continuum theories.

In order to obtain steady-state shock-wave profiles for the reference HM solution ($\delta_1 \geqslant 0, \delta_2 \equiv 0$), we solve the particle-velocity and temperature equations by first-order finite differences. Note that the integration is backwards in the coordinate, i.e., the integration step Δx is negative, since the piston, located far to the right, is the cause of the left-moving shock wave (and in any event, the cold temperature provides nothing much to integrate):

$$\frac{du}{dx} = -\frac{P_0 + \rho_0 u_s^2\left(1 - \frac{u}{u_s}\right) - P(\rho,T)}{\eta_L(\rho,T)}, \tag{5a}$$

$$\frac{dT}{dx} = \frac{\rho_0 u_s\left[E(\rho,T) - \frac{1}{2}(u_s - u)^2 - E_0 - \frac{P_0}{\rho_0}\left(1 - \frac{u}{u_s}\right)\right]}{\kappa(\rho,T)\left[1 - \delta_1\tau_c(\rho,T)\frac{du}{dx}\right]}. \tag{5b}$$

In the LJ fluid, the conditions at the hot end of the shock wave are given by solving iteratively for the Hugoniot jump conditions, while in the ideal-gas case, the EOS is analytic. We identify the origin of the steady shock front in the LJ fluid with the halfway point between cold (u_s) and hot ($u_s - u_p$) particle velocities, as is commonly done in NEMD shock-wave simulations; for the ideal gas, we can choose the peak in T_{xx} as the shock front, since that point is common to all continuum solutions for strong shocks and is nevertheless close to the average of the hot and cold fluid velocities, as well as the maximum (negative) velocity gradient.

III. GENERALIZED CATTANEO-MAXWELL RELAXATION APPLIED TO SHOCK WAVES

In this paper, we take an approach to the relaxation process in continuum hydrodynamics that differs from all earlier Cattaneo-Maxwell treatments [6]. This (*generalized*) Cattaneo-Maxwell approach produces a *relaxed* solution for the five hydrodynamic fields, ρ, T, and $\mathbf{u}$, by taking an independent, previously computed *reference* solution, i.e., $\rho_{\rm ref}$, $T_{\rm ref}$, and $\mathbf{u}_{\rm ref}$, and performing an extra time integration over its exponentially damped past history. For example, we can apply the generalized Cattaneo-Maxwell approach to the temperature field:

$$\begin{aligned} &\frac{\partial T}{\partial t} = -\frac{T(\mathbf{x},t) - T_{\rm ref}(\mathbf{x},t)}{\tau} \qquad \text{(Maxwell)}, \\ &T(\mathbf{x},t) + \tau\frac{\partial T}{\partial t} = T_{\rm ref}(\mathbf{x},t) \qquad \text{(Cattaneo)}, \\ &\Rightarrow T(\mathbf{x},t) = \int_0^\infty ds\, e^{-s} T_{\rm ref}(\mathbf{x}, t - s\tau), \end{aligned} \tag{6a}$$

where τ is the exponential relaxation time; the first line is the usual form of Maxwell relaxation, the second is Maxwell rearranged in the style of Cattaneo, and the third is the formal integral solution. We emphasize that the relaxation is for hydrodynamic fields, rather than fluxes, as we will discuss in more detail later.

The time dependence of temperature relaxation, as outlined in Eq. (6a), is shown schematically in Fig. 1(a), which could represent, for example, either the passage of a shock wave through a fluid initially at temperature T_0 as it reaches the final shocked temperature T_1, or the transient response of fluid located between hot and cold reservoirs as temperature rises from T_0 and approaches the appropriate steady-state (linear-profile) value T_1. By construction, the maximum time derivative at the midpoint of the temperature rise is $\Delta T/\Delta t_{\rm rise} = (T_{\rm ref} - T)/\tau$, so that $\tau/\Delta t_{\rm rise} = (T_{\rm ref} - T)/\Delta T \ll 1$; this is consistent with the physical requirement that the relaxation time τ be approximately τ_c, the mean atomic collision time in the fluid, as measured at the midpoint of the rise, so that $\Delta t_{\rm rise}$ must be at least a few times τ_c. The relaxed solution T is delayed from $T_{\rm ref}$ (to first order) by a time $\sim\tau$, and the duration, or width of the profile—the shock rise time in the case of a shock wave—is also increased by a like amount. As depicted in Fig. 1(a), $\Delta t_{\rm rise}$ is only a handful of relaxation times, similar to the case for shock waves, and the difference between reference and relaxed solutions $(T_{\rm ref} - T)$ is nontrivial compared to the total temperature rise ΔT; consequently, the highly nonequilibrium relaxation effect is nonlocal in time, and history dependence cannot be ignored. Therefore a single-pass, time-marching integration of the hydrodynamic equations is not feasible: A second relaxation integration, as in the third line of Eq. (6a), is essential.

By analogy with Eq. (6a), we write the generalized Cattaneo-Maxwell exponential relaxation equation for a more complicated function of the hydrodynamic fields, such as the heat flux vector $\mathbf{Q}$, as follows:

$$\left(1+\tau\frac{\partial}{\partial t}\right)\mathbf{Q}(\rho,T,\mathbf{u}\mid\mathbf{x},t) = \mathbf{Q}_{\rm ref}(\rho_{\rm ref},T_{\rm ref},\mathbf{u}_{\rm ref}\mid\mathbf{x},t)$$
$$\Rightarrow \mathbf{Q}(\rho,T,\mathbf{u}\mid\mathbf{x},t) = \int_0^\infty ds\, e^{-s}\mathbf{Q}_{\rm ref}(\rho_{\rm ref},T_{\rm ref},\mathbf{u}_{\rm ref}\mid\mathbf{x},t-s\tau). \quad (6b)$$

If the reference solution is Fourier's law, for example, then the right-hand side of Eq. (6b) is $\mathbf{Q}_{\rm ref} = -\kappa_{\rm ref}\nabla T_{\rm ref}$, where $\kappa_{\rm ref} = \kappa(\rho_{\rm ref},T_{\rm ref})$. This right-hand side has been written heretofore [6] as $-\kappa(\rho,T)\nabla T$, which is strictly correct *only* in the perturbation limit where $\tau/\Delta t_{\rm rise} \to 0$, so that $\rho \to \rho_{\rm ref}$ and $T \to T_{\rm ref}$.[1] While this may seem to be a hair-splitting distinction, such near-equilibrium shortcuts to relaxation processes are not even remotely valid for shock waves, and they can lead to singularities in any resulting single-pass, time-marching integration. Figure 1(b) illustrates relaxation for the heat-flux vector Q, representing, for example, either the passage of a left-moving shock wave through a fluid, or a heat pulse coming from a source to the right.

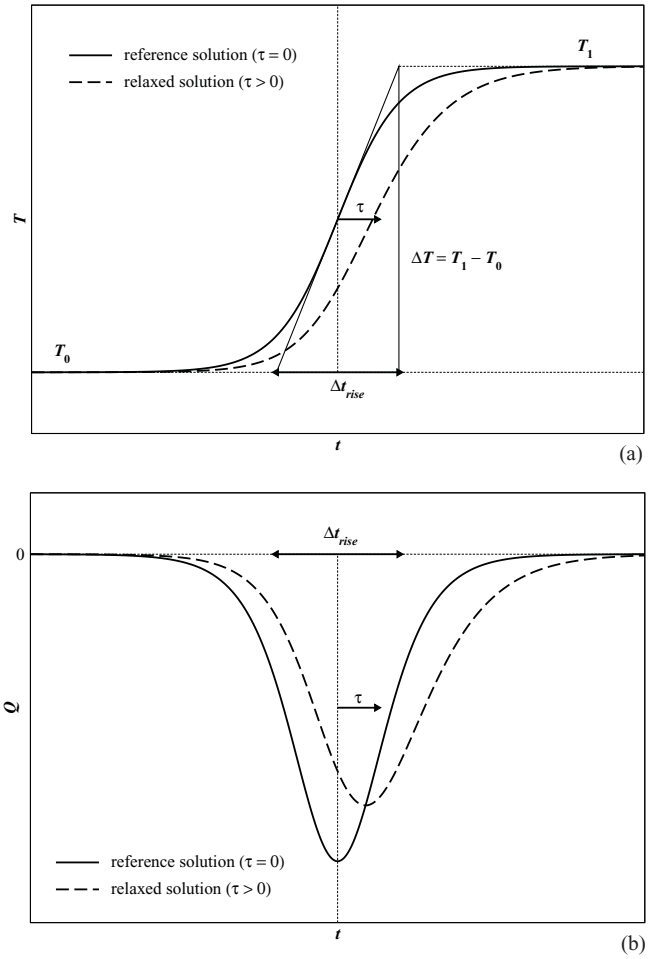

FIG. 1. Schematic of solutions: reference ($\tau = 0$, solid curve) and relaxed ($\tau > 0$, dashed curve) vs time t; (a) temperature T, (b) heat flux Q. Delay time for relaxed solution is $\sim\tau$; rise time (duration) of reference solution $\Delta t_{\rm rise}$ is increased by $\sim\tau$ in the relaxed solution.

Before specializing our generalized relaxation treatment to steady planar shock waves, we note that the Fourier's law relationship between temperature field and heat flux shown in Fig. 1 has a direct analogy in the Navier-Stokes equations, namely, the relationship between fluid velocity (field) and shear stress (flux), as first elucidated by James Clerk Maxwell in 1866. Again, for momentum flux, as in the case of heat flux, the perturbation limit $\tau/\Delta t_{\rm rise} \to 0$ is not valid for shock waves. To go beyond the reference solution of NSF (and also when we include a Burnett-type contribution in HM), an extra integration in time is absolutely essential, particularly for shocks.

In order to describe the relaxation of the kinetic temperature-tensor components in the shock wave, we extend the Navier-Stokes-Fourier plus Burnett (HM) solution for the fluid velocity $u_{\rm ref}$ in Eq. (5a) and the temperature $T_{\rm ref}$ in

[1]Cattaneo's equation in this perturbation limit has often been used to derive the hyperbolic telegrapher's equation for temperature (at constant density and small temperature variations). We can obtain it from the perturbation limit of the partial time derivative of Eq. (6a): $\partial T/\partial t + \tau\partial^2 T/\partial t^2 = \partial T_{\rm ref}/\partial t \to \lambda\nabla^2 T$, where $\lambda = \kappa/\rho C_V$ is the thermal diffusivity (C_V is the constant-volume heat capacity); $\tau = 0$ gives the familiar parabolic Fourier's equation of thermal conduction.

Eq. (5b), so as to include a microscopic Maxwell relaxation process, using the generalized Cattaneo-Maxwell equation introduced in Eq. (1a) and demonstrated schematically in Fig. 1:

$$\frac{\partial u}{\partial t} = -\frac{u - u_{\rm ref}}{\tau_c}, \quad \frac{\partial T}{\partial t} = -\frac{T - T_{\rm ref}}{\tau_T}. \tag{7a}$$

The temporal relaxation of the two hydrodynamic fields occurs on microscopic time scales τ_c and τ_T, which are the mean collision time and a thermal relaxation time, respectively; these relaxation times are not necessarily *identical*, but they cannot physically be too different from each other, either.

Because steady, planar, shock-wave profiles can be transformed to the reference frame of the shock front (recall from Sec. II that the profile coordinate is $x = X + u_s t$), the time derivative in Eq. (7a) can therefore be replaced by the spatial derivative, $\partial/\partial t = u_s d/dx$, and the Cattaneo-Maxwell relaxation equations become

$$\frac{du}{dx} = -\frac{u - u_{\rm ref}}{\lambda_u}, \quad \frac{dT}{dx} = -\frac{T - T_{\rm ref}}{\lambda_T}, \tag{7b}$$

where we have identified the two relaxation lengths $\lambda_u = u_s \tau_c$ and $\lambda_T = u_s \tau_T$, which are somewhat greater than the mean free path between atomic collisions near the middle of the shock front, but still noticeably less than the shock thickness $(u_s \Delta t_{\rm rise})$.

The formal solution to Eq. (7b) for velocity and temperature can be expressed in integral form:

$$\begin{aligned} u(x) &= \int_0^\infty ds\ e^{-s} u_{\rm ref}(x - s\lambda_u), \\ T(x) &= \int_0^\infty ds\ e^{-s} T_{\rm ref}(x - s\lambda_T), \end{aligned} \tag{8a}$$

where Eq. (7b) can be recovered by differentiation with respect to x, followed by partial integration over s. If the reference solution is constant over a number of relaxation lengths (as it is at either the cold or hot end of the shock-wave profile), then the relaxed solution is equal to the reference solution, thereby preserving the Hugoniot jump conditions for both hydrodynamic fields. The solution for u and T can be obtained to third-order accuracy in the spatial integration step Δx by simple recursion, beginning at the cold (left-hand) side of the shock profile:

$$\begin{aligned} u(x + \Delta x) &= u(x) e^{-\Delta x/\lambda_u} \\ &\quad + \frac{\Delta x}{2\lambda_u}[u_{\rm ref}(x + \Delta x) + u_{\rm ref}(x) e^{-\Delta x/\lambda_u}], \\ T(x + \Delta x) &= T(x) e^{-\Delta x/\lambda_T} \\ &\quad + \frac{\Delta x}{2\lambda_T}[T_{\rm ref}(x + \Delta x) + T_{\rm ref}(x) e^{-\Delta x/\lambda_T}]. \end{aligned} \tag{8b}$$

Thus the generalized Cattaneo-Maxwell relaxation integration (in contrast to the original continuum integration for the reference solution itself) is carried out *forward* in time, as shown explicitly in Eq. (8b). We emphasize that the Cattaneo-Maxwell relaxation solution is highly nonlinear, since it depends not just on the coordinate x (or equivalently for the steady shock, time t), but on previous history, i.e., earlier coordinates (or times). While the steady shockwave might appear to involve spatial nonlocality, we emphasize that the nonlocality is actually temporal.

In contrast to HM theory, where we invoked Cattaneo in order to motivate a relaxation term in the heat flux, Burnett-Cattaneo actually relaxes the reference-solution hydrodynamic fields—the velocity and temperature—whose gradients exhibit maxima that precede the response (the maxima of the fluxes) in time. (On the other hand, when transport coefficients are assumed to be independent of density or temperature, i.e., simply constants, it is not surprising to find at the NSF level that maxima of gradients and fluxes coincide [7]; but this is never a realistic assumption.)

Motivated by the HM model for the temperature relaxation in Ref. [1], Hoover and Hoover studied shock propagation in a two-dimensional system of particles interacting by a soft repulsive potential [7]. They assumed constant transport coefficients, and approximated the thermal pressure by a Grüneisen model. Instead of taking advantage of the steady shock-wave condition, the Hoovers supplemented spatial integration of NSF on a staggered mesh with fourth-order Runge-Kutta temporal integration of two temperature relaxation equations. While the idea of going beyond HM temperature relaxation is laudable, the Hoovers' approach involves unnecessary complexity, as well as suffering instabilities, in contrast to the approach we have taken here.

Note that we could have applied Cattaneo-Maxwell relaxation to fluxes, P_{xx} and Q, though the linear relationship between P_{xx} and u makes the relaxation of one identical to the other. However, Q is a function of both u and T [see Eq. (3)], so that, given u (and therefore ρ), one must invert the internal energy E to get T from Q. In the case of the ideal gas, this is a piece of cake, since E is proportional to T; in the case of the dense LJ fluid, inversion of the EOS is not quite so simple, though an iterative search is made feasible by the monotonicity of E as a function of T, at least at high densities and temperatures. We show later that this added complexity of relaxing fluxes, as opposed to fields, is not really necessary.

IV. RESULTS

In Fig. 2, the Navier-Stokes-Fourier, Holian-Mareschal, and Burnett-Cattaneo continuum solutions are compared with nonequilibrium molecular-dynamics simulations for the average temperature T, the longitudinal component of temperature in the shock-wave direction T_{xx}, and the heat-flux vector Q as functions of coordinate x for strong shockwaves in the ideal gas; the same kinds of profiles are displayed in Fig. 3 for a strong shockwave in the Lennard-Jones dense fluid. The profiles for the longitudinal component of the pressure tensor and normal stress difference (i.e., twice the shear stress) are shown in Fig. 4 for the ideal gas and Fig. 5 for the LJ fluid.

The dimensionless Burnett parameter δ_1 in Eq. (3) can be estimated from kinetic theory [8] to be 3.6 for binary collisions of hard spheres; for softer potentials, such as LJ 6–12, the value can be estimated to be about 10% higher. For shocks in dense fluids, binary collisions dominate, so there is no reason to believe that δ_1 would change very much from the hard-sphere ideal-gas value. On the other hand, there is no obvious

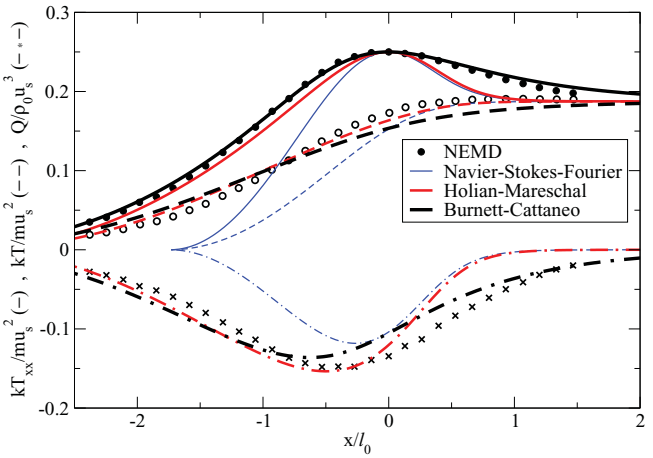

FIG. 2. (Color online) Temperature and heat-flux profiles as functions of position x/l_0 (l_0 is the cold mean free path at the far left-hand side of the shock front) for strong shock waves in the ideal gas; T is the average temperature, T_{xx} is the longitudinal component in the direction of the shock wave, and Q is the heat-flux vector. Nonequilibrium molecular-dynamics (NEMD) simulation data for T_{xx} (solid circles), T (open circles), and Q (X's); Navier-Stokes-Fourier [blue lines (thin black), $\delta_1 = \delta_2 = \lambda_u = \lambda_T = 0$ in Eqs. (3) and (8)]; Holian-Mareschal [red lines (gray), $\delta_1 = 3.6, \quad \delta_2 = 0, \quad \lambda_u = \lambda_T = 0$]; Burnett-Cattaneo, *ab initio* prediction (thick black lines, $\delta_1 = 3.6, \quad \delta_2 = 0, \quad \lambda_u = \lambda_T = 0.77 l_0$).

a priori way to predict for the Holian-Mareschal heat-flux vector what the relaxation parameter δ_2 should be, apart from not being too large compared to 1. For that reason, and since it is an approximation to the relaxation process (while Burnett-Cattaneo provides an *explicit* solution), and since we have found that the Burnett term in the heat flux accounts for the principal effect on the cold compression side of the shock front, we have set $\delta_2 \equiv 0$ in this paper.

The fluid velocity at the shock front is defined in the ideal-gas case to coincide with the peak of T_{xx} (i.e., u is half the shock velocity for a strong shock); therefore a plausible

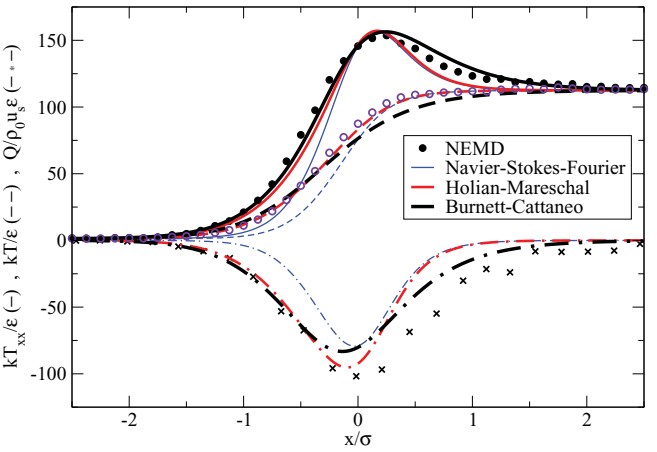

FIG. 3. (Color online) Temperature and heat-flux profiles as functions of position x/σ for a strong shockwave in the dense Lennard-Jones fluid (LJ length unit σ, energy unit ε) [3]; T is the average temperature, T_{xx} is the longitudinal component in the direction of the shockwave, and $Q/\rho_0 u_s$ is the heat-flux vector divided by the constant mass flux $\rho_0 u_s$. Nonequilibrium molecular-dynamics (NEMD) simulation data for T_{xx} (solid circles), T (open circles), and Q (X's); Navier-Stokes-Fourier [blue lines (thin black), $\delta_1 = \delta_2 = \lambda_u = \lambda_T = 0$ in Eqs. (3) and (8)]; Holian-Mareschal [red lines (gray), $\delta_1 = 3.6, \quad \delta_2 = 0, \quad \lambda_u = \lambda_T = 0$]; Burnett-Cattaneo, *ab initio* prediction (thick black lines, $\delta_1 = 3.6, \quad \delta_2 = 0, \quad \lambda_u = \lambda_T = 0.43\sigma$). For the continuum theories, T_{xx} was evaluated from the LJ EOS using Eq. (4). The NEMD profiles for the temperature components are smooth data obtained from simulations with large cross sections [3].

value for the relaxation lengths in the case of the ideal gas is $\lambda_u/l_0 = \lambda_T/l_0 = l/l_0 = \rho_0/\rho = u/u_s = 1/2$, where l is the mean free path at the shock front and l_0 is the value at the cold initial state. We can get a better approximation by evaluating the mean free time near the shock front [1], which gives $\lambda_u/l_0 = u_s \tau_c/l_0 \sim \lambda_T/l_0 = 0.77$, so that the measured shock thickness from NEMD is approximately $3.1\lambda_u$. For

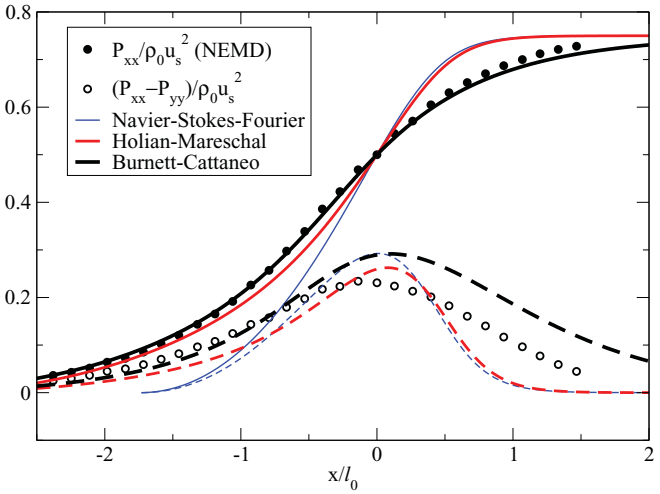

FIG. 4. (Color online) Profiles of the longitudinal pressure component P_{xx} and twice the shear stress $2\tau = P_{xx} - P_{yy}$ for strong shock waves in the ideal gas (scaled by $\rho_0 u_s^2$) (see legend in Fig. 2).

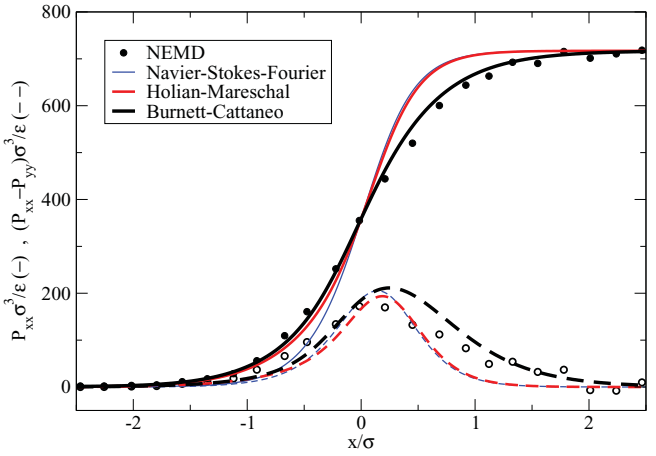

FIG. 5. (Color online) Profiles of the longitudinal pressure component P_{xx} and twice the shear stress $2\tau = P_{xx} - P_{yy}$ for a strong shockwave in the Lennard-Jones dense fluid (in LJ units of ε/σ^3) (see legend in Fig. 3).

the dense LJ fluid, we can evaluate $\lambda_u = u_s\tau_c = u_s\eta_L/B_S$ at the midpoint of the NSF shock front [3], so that $\lambda_u \sim \lambda_T = 0.43\sigma$, whereby the measured shock thickness from NEMD is approximately $3.7\lambda_u$. Because the isothermal sound speed $c_s \sim u_s/2$ in both cases, the true shock thickness is about six times the mean free path, as given by $l = c_s\tau_c$. In the conventional wisdom of the hydrodynamics community, it is shocking that any continuum theory (like Burnett-Cattaneo) could apply so well to shock fronts that are only a handful of mean free paths thick. Apart from the fact that "half a dozen" is demonstrably a large *enough* number, we have no deeper philosophical comment.

As we said in the previous section, one could apply the Cattaneo-Maxwell relaxation to the heat flux Q, rather than the temperature T, though such an approach is more complicated because of the need to invert the internal energy to get the temperature. In fact, the resulting shock profiles are somewhat worse than in the preceding figures, so that the extra effort is unwarranted. Also, relaxing the stress is identical to relaxing the fluid velocity, since the two are linearly related to each other; as a result, we find indeed that T_{xx} and P_{xx} show no differences whatsoever when fluxes are relaxed, rather than fields.

The continuum modeling by HM theory is noticeably better than NSF, but it still suffers from a defect that we had noted earlier in Refs. [1] and [3]: In both the ideal gas and the dense LJ fluid, the continuum prediction of the relaxation of the profiles on the hot side of the shock front is too rapid, with NSF and HM theories being strikingly similar in that regard. On the other hand, the Burnett nonlinear term in HM theory accounts quite well for the shock compression on the cold side of the shock front, when compared to NEMD, while NSF is not at all satisfactory on this score. What is particularly notable is that the relaxation mechanism, represented by our generalized Cattaneo-Maxwell integration of the reference Burnett solution (Burnett-Cattaneo), gives continuum shock-wave profiles that are very close to NEMD, even for the so-called "*ab initio*" choices for the relaxation lengths. Obviously, if one were to "fine tune" the values of δ_1, λ_u, and λ_T, the resulting theory would become almost quantitative for strong shocks.

V. CONCLUSIONS

The heat-flow equation proposed earlier by Holian and Mareschal [1], based on studies of shock waves in the ideal gas, and tested further for dense fluids [3], can be improved upon by using the generalized Cattaneo-Maxwell exponential relaxation equation [Eqs. (8)], as applied to hydrodynamic fields in planar steady shock waves—fluid velocity u and average temperature T—provided that the fields are the solutions to Navier-Stokes [Eq. (5a)] and Fourier's law of heat conduction, as augmented by a nonlinear Burnett strain-rate-dependent conductivity [Eq. (5b)]. The unrelaxed NSF plus Burnett shock profiles describe the cold compressive side of the profiles better than NSF alone, but neither describes the slow relaxation from the shock front to the final hot, shocked state. The nonlinear generalized Cattaneo-Maxwell integration with constant relaxation lengths is the *essential* component to a continuum description of the temperature relaxation to the final state, as seen in NEMD shock-wave simulations.

We recapitulate the important features of our new Burnett-Cattaneo continuum theory: (i) An enhancement of the thermal conductivity by strain rate, a nonlinear feature common to the Burnett expansion beyond Navier-Stokes-Fourier, is crucial to the early-time shock rise on the cold side of the front. (ii) An additional relaxation time integration that brings the longitudinal component of temperature (in the shock direction) into equilibrium with the transverse components is critical to describing the late-time relaxation on the hot side of the shock front. The velocity and temperature fields of the reference solution (NSF continuum theory with the Burnett heat-flux term) are integrated over their exponentially damped past history, using *a priori* estimates for constant relaxation lengths obtained from the EOS and NSF transport coefficients.

Among all the continuum theories we have applied to the shock problem, Burnett-Cattaneo is *uniquely* able to capture the NEMD shock thickness as well as magnitudes of the fluxes. Continuum Burnett-Cattaneo shock profiles are *almost* quantitative throughout in their faithfulness to atomistic shock-wave simulations. Even though the shock thicknesses are only a handful of mean free paths, it would appear that complexity beyond the Burnett-Cattaneo level would bring only marginal improvement. The generalized Cattaneo-Maxwell approach we have presented here can be applied to other temporally nonlocal phenomena, including relaxation of internal degrees of freedom of polyatomic molecules under strong external driving.

ACKNOWLEDGMENTS

John Barber helped us to clarify some aspects of the derivations presented here. We recognize the profound significance of Bill Hoover's insistence some thirty-two years ago (in spite of conventional wisdom at the time) that the most stringent test of continuum theory is provided by shock waves: Shocks have shown us—at last—how to go beyond linear Navier-Stokes-Fourier theory.

[1] B. L. Holian and M. Mareschal, Phys. Rev. E **82**, 026707 (2010).

[2] E. Salomons and M. Mareschal, Phys. Rev. Lett. **69**, 269 (1992); B. L. Holian, C. W. Patterson, M. Mareschal, and E. Salomons, Phys. Rev. E **47**, R24 (1993).

[3] B. L. Holian, M. Mareschal, and R. Ravelo, J. Chem. Phys. **133**, 114502 (2010).

[4] V. Y. Klimenko and A. N. Dremin, in *Detonatsyia Chernogolovka*, edited by O. N. Breusov *et al.* (Akademik Nauk, Moscow, 1978), p. 79; W. G. Hoover, Phys. Rev. Lett. **42**, 1531 (1979); B. L. Holian, W. G. Hoover, B. Moran, and G. K. Straub, Phys. Rev. A **22**, 2798 (1980).

[5] For an excellent review of alternative temperature definitions in nonequilibrium situations, see J. Casas-Vazques and D. Jou, Rep. Prog. Phys. **66**, 1937 (2003).

[6] C. Cattaneo, C. R. Hebd. Seances Acad. Sci. **247**, 431 (1958); Applications of Cattaneo-Maxwell relaxation: M. E. Gurtin and A. C. Pipkin, Arch. Ration. Mech. Anal. **31**, 113 (1968); S. L. Sobolev, Sov. Phys. Usp. **34**, 217 (1991); Reviews: D. D. Joseph and L. Preziosi, Rev. Mod. Phys. **61**, 41 (1989); **62**, 375 (1990); D. Jou, J. Casas-Vazquez, and G. Lebon, *Extended Irreversible Thermodynamics* (Springer, Berlin, 1993); I. Müller and T. Ruggeri, *Rational Extended Thermodynamics* (Springer-Verlag, New York, 1998).

[7] W. G. Hoover and C. G. Hoover, Phys. Rev. E **81**, 046302 (2010).

[8] C. S. Wang Chang and G. E. Uhlenbeck, *Studies in Statistical Mechanics*, edited by J. de Boer and G. E. Uhlenbeck (North-Holland, Amsterdam, 1970), vol. 5, p. 7.